Title

Contour dynamics method for solving the Grad-Shafranov equation with applications to high beta equilibria

Journal

Physics of Plasmas, 11

Authors

Gourdain, P A
Leboeuf, J.-N.

Publication Date

2004

Peer reviewed

Contour dynamics method for solving the Grad–Shafranov equation with applications to high beta equilibria

P.-A. Gourdain[a] and J.-N. Leboeuf
Department of Physics and Astronomy, University of California, Los Angeles, California 90095-1547

(Received 8 October 2003; accepted 1 June 2004; published 20 August 2004)

Numerous methods exist to solve the Grad–Shafranov equation, describing the equilibrium of a plasma confined by an axisymmetric magnetic field. Nevertheless, they are limited to low beta or small plasma pressure. Combining a nonconservative variational principle with a contour dynamics approach, the approach presented in this paper converges for extreme high beta configurations. By reducing the dimension of the problem from two to one, a compact and efficient numerical algorithm can be developed, and a wide range of boundary shapes can be utilized. Furthermore, the iterative nature of this technique greatly facilitates convergence at high beta while minimizing computation times. © *2004 American Institute of Physics*. [DOI: 10.1063/1.1776174]

I. INTRODUCTION

Stable high beta plasmas in magnetic confinement devices such as tokamaks and stellarators[1] can transform magnetic fusion into a clean and abundant source of energy. To reach such a goal, magnetohydrodynamics (MHD) equilibrium codes are the most basic and primordial assets.

Numerous methods exist to solve the so-called Grad–Shafranov (GSh) equation,[2] describing the ideal MHD equilibrium of an axisymmetric plasma confined by a magnetic field. Due to the nonlinearity of this equation, all numerical methods solving for a given plasma equilibrium are iterative.[3] Two different types of numerical codes exist. The first sort is based on an Eulerian scheme, relying on a two-dimensional (2D) mesh without any direct link to plasma shape or properties.[4,5] The second one is based on a Lagrangian scheme using curvilinear flux coordinates to map plasma geometry,[6] involving adaptive grid,[7] variational,[8] or perturbative approaches,[9] or inverse coordinates[10] methods. Nevertheless, many of these excellent methods cannot compute asymptotic high beta equilibria such as the one presented at the end of this paper.

The technique presented in this publication computes high plasma beta equilibria with large outward shifts of the magnetic axis or Shafranov shifts, while maintaining computational efficiency.[11] By changing coordinate systems from geometric space to flux space, the dimension of the derivative operator in the GSh is effectively reduced by one. This has an important implication: a set of contours, yielding a single gradient coordinate, can now replace an area yielding two gradient coordinates for each quantity involved in the equation. This technique is known in fluid dynamics as the contour dynamics method.[12] This is a generalized case of the water-bag method introduced by Berk and Roberts.[13] Potter[14] used such a method to solve the GSh equation along with a flux conserving variational principle, restricting it to a limited set of low beta equilibria. Rosenbluth *et al.*[15] applied an equivalent scheme to study the nonlinear evolution of kink modes in tokamaks. By coupling of a nonconservative variational principle to the contour dynamics method, a simple one-dimensional iteration scheme can efficiently converge to an equilibrium solution at high beta.[16]

The remainder of this paper is organized as follows: In Sec. II, the GSh equation is computed in flux space and an intuitive approach to the contour dynamics principle introduces the basic idea of the method described in this paper; then, the algorithm to solve the GSh equation is presented in Sec. III; numerical results obtained with this technique, in particular for high beta plasma equilibria, are given in Sec. IV; while Sec. V contains conclusions.

II. THE CONTOUR DYNAMICS APPLIED TO IDEAL MHD

A. The Grad–Shafranov equation in flux space

The equilibrium of a perfectly conductive plasma confined by an axisymmetric magnetic field is usually given by the equation of Grad–Shafranov[2] (GSh). This equation describes the local equilibrium between the force arising from the static pressure of the fluid and the magnetic force locally applied. The surfaces of constant pressure are actually nested surfaces. The pressure increases from the interface plasma-vacuum to the center of the plasma, called magnetic axis, where it reaches a maximum. Figure 1 illustrates such a configuration, in the vertical plane (R,Z,ϕ). In this plane of symmetry, the ideal magneto hydrodynamics equilibrium of a plasma can be reduced to

$$\frac{\partial}{\partial R}\left(\frac{1}{R}\frac{\partial \psi}{\partial R}\right)+\frac{1}{R}\frac{\partial^2 \psi}{\partial Z^2}=-\left(\mu R\frac{dp}{d\psi}+\frac{1}{2R}\frac{dF^2}{d\psi}\right) \quad \text{or}$$
$$\Delta^* \psi=-\left(\mu R\frac{dp}{d\psi}+\frac{1}{2R}\frac{dF^2}{d\psi}\right). \tag{1}$$

ψ stands for the flux of the poloidal induction B_p in the plane $Z=0$. p is the pressure inside the fluid. F, the toroidal function,[17] represents the net poloidal current crossing the plane $Z=0$. Furthermore p and F are functions of ψ only.[2] The presence of ψ on both left-hand and right-hand sides

[a]Electronic mail: gourdain@ucla.edu

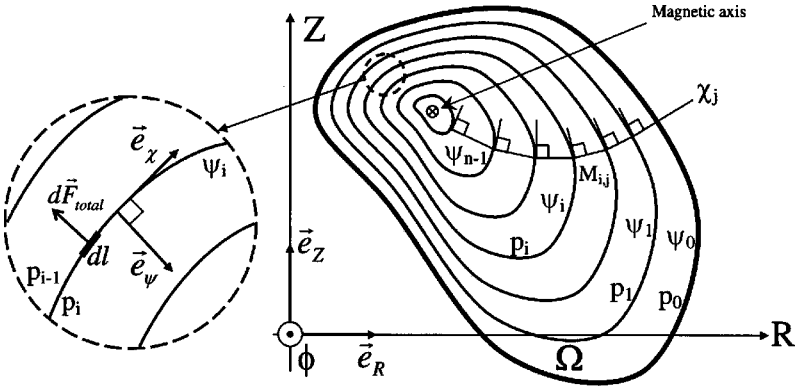

FIG. 1. Cylindrical coordinate system (R, Z, ϕ) and flux coordinate system (ψ, χ, ϕ).

makes this elliptic partial differential equation nonlinear. Only iterative methods can solve this kind of problem. Several efficient schemes[18,19] exist to find a solution for a given pressure and toroidal function distribution.

Another difficulty in this equation arises from the complex form of the operator Δ^*. The (R,Z) coordinate system does not take advantage of the topology of the solution. One can try to experiment with other coordinate systems in an attempt to simplify this equation. A simple choice is to map the nested isobar surfaces. Because p is a function of the flux ψ only, the surfaces of constant pressure are also surfaces of constant flux ψ. It is possible to build a new coordinate system, based on flux surfaces, by using three new vectors as e_ψ, e_χ, e_ϕ defined as follows:

- the ψ direction, given by e_ψ, is orthogonal to the flux surfaces in each point,
- e_ϕ is the vector defining the ignorable toroidal direction,
- the χ direction is given by $e_\chi = e_\phi \times e_\psi$.

These vectors define an orthogonal coordinate system (ψ, χ, ϕ), called "flux space,"[14] shown in Fig. 1. This space is not metric, and by using the distance invariance principle, we obtain Eq. (2) in the geometric space (R, Z, ϕ) and the flux space (ψ, χ, ϕ). Figure 2 illustrates the similarity between the distance dr and h^ψ along the ψ direction

$$d\vec{r}^2 = (h^\psi d\psi)^2 + (h^\chi d\chi)^2 + (Rd\phi)^2,$$

$$d\vec{r}^2 = (dR)^2 + (dZ)^2 + (Rd\phi)^2. \tag{2}$$

After defining the coordinate system, we can now derive the revised form of the GSh equation in flux space (ψ, χ, ϕ). The magnetic induction is always derived from the flux and the toroidal function,

$$\vec{B} = \vec{B}_\phi + \vec{B}_p \text{ with } \vec{B}_p = \frac{1}{R} \nabla \psi \times \vec{e}_\phi \text{ and } \vec{B}_\phi = \frac{F(\psi)}{R} \vec{e}_\phi. \tag{3}$$

Using the formula of the ∇ operator given in the Appendix, we have

$$\vec{B} = \frac{F(\psi)}{R} \vec{e}_\phi - \left(\frac{1}{Rh^\psi} \right) \vec{e}_\chi \text{ with } \vec{B}_p = -\left(\frac{1}{Rh^\psi} \right) \vec{e}_\chi. \tag{4}$$

Maxwell's equations give the current density from the curl of Eq. (4),

$$\mu \vec{J} = -\frac{1}{Rh^\psi} \frac{dF(\psi)}{d\psi} \vec{e}_\chi - \frac{1}{h^\psi h^\chi} \frac{\partial \frac{h^\chi}{Rh^\psi}}{\partial \psi} \vec{e}_\phi. \tag{5}$$

Then, by using the classical static equilibrium equation (6) between pressure gradient and current flow,

$$\vec{\nabla} p = \vec{J} \times \vec{B}, \tag{6}$$

we obtain

$$\frac{1}{h^\psi h^\chi} \frac{\partial \frac{h^\chi}{Rh^\psi}}{\partial \psi} = -\left(\mu R \frac{dp}{d\psi} + \frac{1}{2R} \frac{dF^2}{d\psi} \right) \text{ or} \tag{7}$$

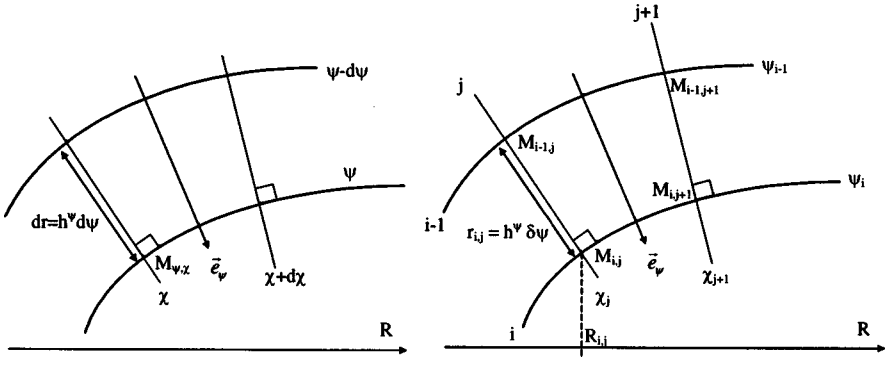

FIG. 2. Detail of the continuous and discrete flux space (ψ, χ).

$$\mu J_\phi = \mu R \frac{dp}{d\psi} + \frac{1}{2R}\frac{dF^2}{d\psi}.$$

Equation (7) is the GSh equation in flux space. By changing coordinate systems, we effectively reduced the dimension of the derivative operator from two to one. This has an important implication: a set of contours, yielding a single-coordinate gradient, can now replace an area, yielding a two-coordinate gradient, for each quantity involved in the equation. This technique is known in fluid dynamics as the contour dynamics method.[12] Despite the nonlinearity of Eq. (7), a simple one-dimensional iteration scheme can converge to a solution. Using this coordinate system, the following paragraphs introduce the contour dynamics idea.

B. Physical interpretation of the contour dynamics scheme

To understand the method depicted in this paper, it is best to look at a discrete set of nested surfaces $(p_0, \ldots, p_n)$, or $(\psi_0, \ldots, \psi_n)$. If we take an isobar surface i at random in the distribution from Fig. 1 and we look at the group of forces that exists on both sides of this surface we have

$$d\vec{F}_{\text{total}} = -2\pi R dl([p + p_{\text{magnetic}}]_i - [p + p_{\text{magnetic}}]_{i-1})\vec{e}_\psi, \quad (8)$$

where dl represents an infinitesimal portion of the flux surface along the χ direction. The index i refers to the pressure on the inside area of the surface i and $i-1$ to the pressure on the outside area of the same surface i. Between surfaces, the pressure is assumed to be constant. In this framework, we can develop Eq. (8) by replacing the value of the magnetic pressure by the toroidal and poloidal inductions from Eq. (4),

$$d\vec{F}_{\text{total}} = -\left[p + \frac{1}{2\mu}\left(\frac{1}{Rh^\psi}\right)^2 + \frac{1}{2\mu}\left(\frac{F}{R}\right)^2\right]_{i-1}^{i} 2\pi R dl \vec{e}_\psi. \quad (9)$$

We can introduce the linear operator δ which expresses the difference of any function f on both sides of a flux surface. δ has two remarkable properties:

(1) if f is continuous across a flux surface then $\delta f = 0$ across this surface;
(2) $\delta fg = \langle f\rangle \delta g + \langle g\rangle \delta f$, where $\langle\cdot\rangle$ represents the average of a function across the surface.

After some rearrangements, Eq. (10) replaces Eq. (9),

$$d\vec{F}_{\text{total}} = -\frac{\delta\psi}{\mu} 2\pi dl \vec{\zeta} \quad \text{with}$$
$$\vec{\zeta} = \left(\frac{1}{\delta\psi}\left\langle\frac{1}{h^\psi}\right\rangle \delta\left(\frac{1}{Rh^\psi}\right) + \mu R\frac{\delta p}{\delta\psi} + \frac{1}{2R}\frac{\delta(F^2)}{\delta\psi}\right)\vec{e}_\psi. \quad (10)$$

If we wish to approximate $\langle\cdot\rangle$ by its value on one side of the surface then we have

$$\vec{\zeta} = \left(\frac{1}{h^\psi \delta\psi}\delta\left(\frac{1}{Rh^\psi}\right) + \mu R\frac{\delta p}{\delta\psi} + \frac{1}{2R}\frac{\delta(F^2)}{\delta\psi}\right)\vec{e}_\psi. \quad (11)$$

At the equilibrium, the total force density dF_{total} is null and we obtain

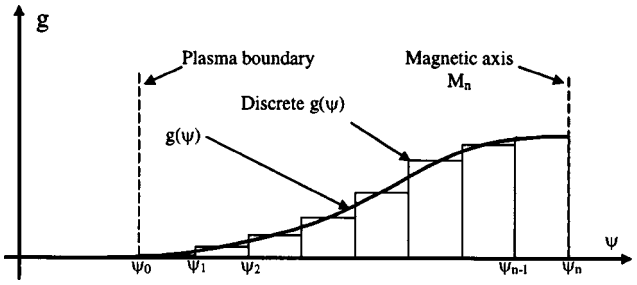

FIG. 3. Discretization of a continuous function g on the discrete flux space.

$$\frac{1}{h^\psi \delta\psi}\delta\left(\frac{1}{Rh^\psi}\right) + \mu R\frac{\delta p}{\delta\psi} + \frac{1}{2R}\frac{\delta(F^2)}{\delta\psi} = 0 \quad \text{or } \vec{\zeta} = \vec{0}. \quad (12)$$

Equation (12) represents the GSh equilibrium configuration in the discrete case, which is an approximation of the continuous case of Eq. (7). So the contour dynamics scheme describes the static equilibrium of a set of contours in an appropriate local coordinate system, i.e., on the flux surface itself, thus reducing the dimension of the GSh equation. A more rigorous mathematical demonstration follows this intuitive introduction where Eq. (11) will appear again.

The following sections present the algorithm based on the contour dynamics method and its practical application for high beta solutions. Due to the axisymmetric nature of the problem, we will refer to "flux surfaces" as "flux lines" in many occasions.

III. CONVERGENCE ALGORITHM

In this section, we construct an original algorithm that solves Eq. (7) using a nonconservative variational principle, which cannot be compared to an energy minimization principle usually found in many variational methods.[14] After the definition of an error between the LHS and the RHS of the GSh equation, an error reduction scheme, a numerical viscosity that controls convergence and a flux correction are presented.

A. Error definition

We define an error $\zeta(\psi, \chi, R)$ between the RHS and LHS of Eq. (7) for all points of our domain of definition Ω so we can monitor the progress of the algorithm in solving for the sought solution,

$$\zeta(\psi,\chi,R) = \frac{1}{h^\psi h^\chi}\frac{\partial\dfrac{h^\chi}{Rh^\psi}}{\partial\psi} + \left(\mu R\frac{dp}{d\psi} + \frac{1}{2R}\frac{dF^2}{d\psi}\right). \quad (13)$$

At the equilibrium $\zeta(\psi, \chi, R)$ is null everywhere inside the plasma. For all practical purposes, the problem must be solved on a grid. A discrete set of coordinates $(\psi_0, \psi_1, \ldots \psi_n)$ is used to number our series of nested flux surfaces, as illustrated in Fig. 1. p and F will be considered constant between each contour $\psi = \psi_i$, as prescribed by the contour dynamics discretization principle, presented in Fig. 3. At this point, areas between lines can be ignored as we adopt a one-dimensional point of view. In the rest of the paper we will

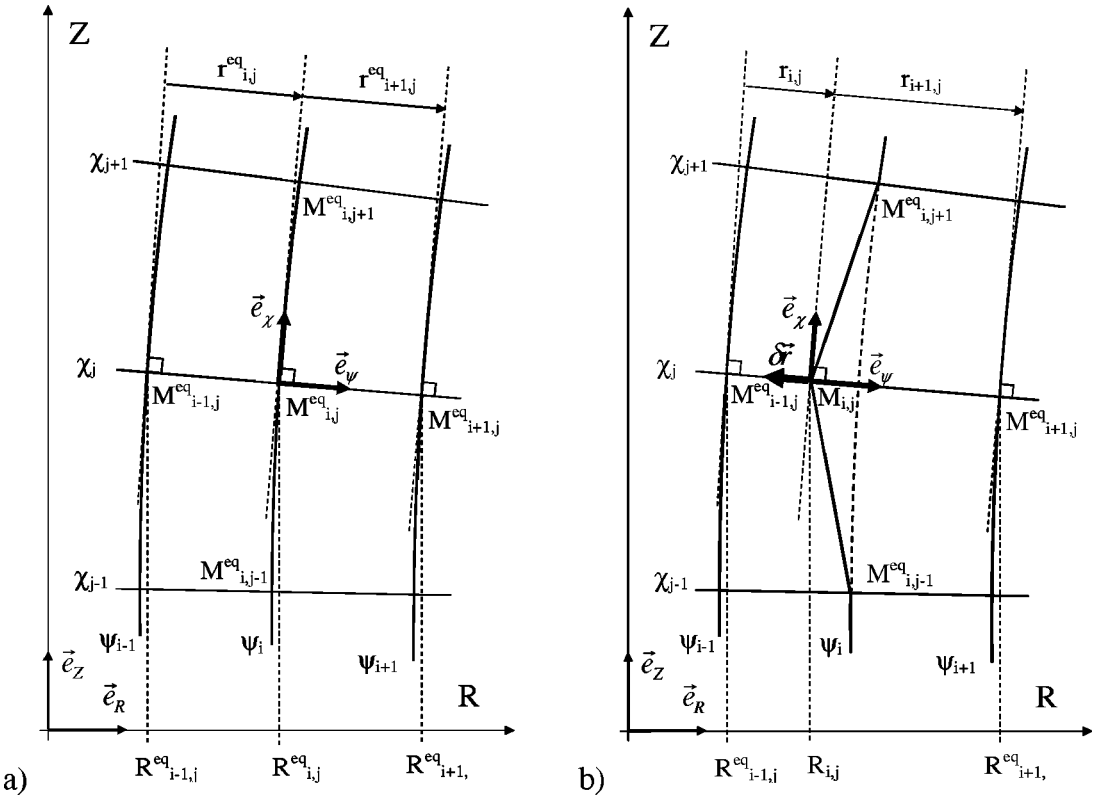

FIG. 4. (a) Detail view of the equilibrium configuration, (b) infinitesimal displacement δr giving $M_{i,j}$ by moving $M^{eq}_{i,j}$.

use the index i to number the ψ contours and j to number the χ lines. At each point $M^{\psi\chi}_{i,j}(\psi_i,\chi_j)$ of the flux space corresponds a unique point $M^{RZ}_{i,j}(R_{i,j},Z_{i,j})$ of the geometric space. Because of their trivial correspondence, we will never distinguish between them and always use $M_{i,j}$. Across each contour in $M_{i,j}$, Eq. (13) may be transformed into

$$\zeta_{i,j}=\frac{1}{h^\psi h^\chi \delta\psi}\delta\left(\frac{h^\chi}{Rh^\psi}\right)+\left(\mu R\frac{\delta p}{\delta\psi}+\frac{1}{2R}\frac{\delta(F^2)}{\delta\psi}\right). \tag{14}$$

Across each ψ contour, h^ψ is discontinuous while h^χ is continuous. On the other end, h^χ is discontinuous while h^ψ is continuous across the χ lines. As discussed earlier, the δ operator acts only on discontinuous variables across ψ contours, so h^χ disappears from Eq. (14) when discretized and we have

$$\zeta_{i,j}=\frac{1}{h^\psi \delta\psi}\delta\left(\frac{1}{Rh^\psi}\right)+\left(\mu R\frac{\delta p}{\delta\psi}+\frac{1}{2R}\frac{\delta(F^2)}{\delta\psi}\right). \tag{15}$$

If we recall Eq. (10), dF_{total} and $\zeta_{i,j}$ are actually proportional. So this error can be interpreted as the net force applied to each point $M_{i,j}$ of the flux lines, within a factor R_{ij}. When the error is null, the force on the surface is null and the static equilibrium has been found. We can also give a physical interpretation to h^ψ which corresponds to the distance between two neighboring contours in flux space. Equation (2) gives $dr=h^\psi d\psi$ along the ψ direction of the continuous domain, illustrated in Fig. 2 and in the discrete case, we have

$$r_{i,j}=h^\psi_{i,j}(\psi_i-\psi_{i-1}). \tag{16}$$

By replacing h^ψ in Eq. (15) we obtain Eq. (17) for all points inside the plasma,

$$\zeta_{i,j}=\frac{1}{r_{i,j}}\left(\frac{\psi_{i+1}-\psi_i}{r_{i+1,j}R_{i+1,j}}-\frac{\psi_i-\psi_{i-1}}{r_{i,j}R_{i,j}}\right)+\left[\mu R\frac{\delta p}{\delta\psi}+\frac{1}{2R}\frac{\delta(F^2)}{\delta\psi}\right]_{i,j}. \tag{17}$$

This represents the discrete form of the error defined by Eq. (13). The variable χ actually disappeared from the equation. The following paragraphs detail the utilization of this error in the construction of the algorithm, where the χ coordinate will be ignored altogether.

B. Error reduction

The core of the method focuses on minimizing the error $|\zeta_{i,j}|$ for each point of the plasma M_{ij}. Before working on such a complicated task, it is natural to look at a simple case first. We suppose the solution to the GSh equation has been found. A detail view of the equilibrium configuration is shown in Fig. 4(a). All points $M^{eq}_{i,j}$ of the plasma verify

$$\frac{1}{r^{eq}_{i,j}}\left(\frac{\psi_{i+1}-\psi_i}{r^{eq}_{i+1,j}R^{eq}_{i+1,j}}-\frac{\psi_j-\psi_{j-1}}{r^{eq}_{i,j}R^{eq}_{i,j}}\right)=-\left[\mu R\frac{\delta p}{\delta\psi}+\frac{1}{2R}\frac{\delta(F^2)}{\delta\psi}\right]^{eq}_{i,j}. \tag{18}$$

We now introduce a small perturbation δr by slightly moving a single-point $M^{eq}_{i,j}$ from its original equilibrium po-

sition. It is reasonable to assume that a displacement along the χ direction will not affect the error, because it is independent of this variable. Therefore, only displacements along the ψ direction will be considered in this exploratory demonstration. Such a displacement, orthogonal to the ψ flux contour, takes the form of

$$\delta\vec{r} = \delta r \,.\, \vec{e}_{\psi}. \tag{19}$$

This infinitesimal displacement transforms $M_{i,j}^{eq}$ into $M_{i,j}$, as shown in Fig. 4(b). By inserting Eq. (18) into Eq. (17) we obtain

$$\zeta_{i,j} = \frac{1}{r_{i,j}}\left(\frac{\psi_{i+1}-\psi_i}{r_{i+1,j}R_{i+1,j}^{eq}} - \frac{\psi_i-\psi_{i-1}}{r_{i,j}R_{i,j}}\right) - \frac{1}{r_{i,j}^{eq}}\left(\frac{\psi_{i+1}-\psi_i}{r_{i+1,j}^{eq}R_{i+1,j}^{eq}} - \frac{\psi_i-\psi_{i-1}}{r_{i,j}^{eq}R_{i,j}^{eq}}\right). \tag{20}$$

The values of $r_{i,j}$, $r_{i+1,j}$, and $R_{i,j}$ come from Eq. (21) in vectorial or algebraic forms,

$$r_{i,j}\vec{e}_{\psi} = r_{i,j}^{eq}\vec{e}_{\psi} + \delta\vec{r}, \quad r_{i,j} = r_{i,j}^{eq} + \delta r,$$

$$r_{i+1,j}\vec{e}_{\psi} = r_{i+1,j}^{eq}\vec{e}_{\psi} - \delta\vec{r}, \quad r_{i+1,j} = r_{i+1,j}^{eq} - \delta r,$$

$$R_{i,j}\vec{e}_{R} = R_{i,j}^{eq}\vec{e}_{R} + \delta\vec{r}, \quad R_{i,j} = R_{i,j}^{eq} + \delta r\cos(\vec{e}_{\psi},\vec{e}_{R}). \tag{21}$$

Because δr is infinitesimal, it is possible to approximate $1/r_{i,j}$, $1/r_{i+1j}$, and $1/R_{i,j}$ by using Taylor's expansions given by

$$\frac{1}{r_{i,j}} = \frac{1}{r_{i,j}^{eq}}\frac{1}{1+\dfrac{\delta r}{r_{i,j}^{eq}}} = \frac{1}{r_{i,j}^{eq}}\left[1 - \frac{\delta r}{r_{i,j}^{eq}} + O(\delta r^2)\right],$$

$$\frac{1}{R_{i,j}} = \frac{1}{R_{i,j}^{eq}}\frac{1}{1+\dfrac{\delta r}{R_{i,j}^{eq}}\cos(\vec{e}_{\psi},\vec{e}_{R})} = \frac{1}{R_{i,j}^{eq}}\left[1 - \frac{\delta r}{R_{i,j}^{eq}}\cos(\vec{e}_{\psi},\vec{e}_{R}) + O(\delta r^2)\right],$$

$$\frac{1}{r_{i+1,j}} = \frac{1}{r_{i+1,j}^{eq}}\frac{1}{1-\dfrac{\delta r}{r_{i+1,j}^{eq}}} = \frac{1}{r_{i+1,j}^{eq}}\left(1 + \frac{\delta r}{r_{i+1,j}^{eq}} + O(\delta r^2)\right). \tag{22}$$

If we incorporate the results of Eq. (22) into Eq. (20) we have

$$\zeta_{i,j} = K_{i,j}\delta r + O(\delta r^2) \quad \text{with} \tag{23}$$

$$K_{i,j} = \frac{1}{r_{i,j}^{eq}}\left[\left(\frac{1}{r_{i+1,j}^{eq}} - \frac{1}{r_{i,j}^{eq}}\right)\frac{\psi_{i+1}-\psi_i}{r_{i+1,j}^{eq}R_{i+1,j}^{eq}} + \left[\frac{2}{r_{i,j}^{eq}} + \frac{\cos(\vec{e}_{\psi},\vec{e}_{R})}{R_{i,j}^{eq}}\right]\frac{\psi_i-\psi_{i+1}}{r_{i,j}^{eq}R_{i,j}^{eq}}\right].$$

Furthermore, Eq. (18) leads to a new analytic expression of $K_{i,j}$ where the current density appears,

$$K_{i,j} = \frac{1}{r_{i,j}^{eq}}\left[\frac{1}{r_{i+1,j}^{eq}}\frac{\psi_{i+1}-\psi_i}{r_{i+1,j}^{eq}R_{i+1,j}^{eq}} + \left[\frac{1}{r_{i,j}^{eq}} + \frac{\cos(\vec{e}_{\psi},\vec{e}_{R})}{R_{i,j}^{eq}}\right]\times\frac{\psi_i-\psi_{i-1}}{r_{i,j}^{eq}R_{i,j}^{eq}} + \mu J_{\phi_{i,j}}\right] > 0. \tag{24}$$

Because ψ increases with i, all factors of $K_{i,j}$ are positive and any infinitesimal displacement δr changing the position of $M_{i,j}$ can be defined by the error $\zeta_{i,j}$ as

$$\delta\vec{r} = \frac{1}{K_{i,j}}\vec{\zeta}_{i,j} + O(\delta r^2)\vec{e}_{\psi}, \quad \text{where } \vec{\zeta}_{i,j} = \zeta_{i,j}\vec{e}_{\psi}. \tag{25}$$

The preceding equation reveals that any random infinitesimal displacement δr is proportional to the vectorial error $\zeta_{i,j}$ it generated, and they both have the same orientation along the ψ direction. The major implication arises when δr is actually unknown. In this case, $K_{i,j}$ cannot be computed. Nevertheless, $K_{i,j}$ is not a function of δr and can be considered constant. Because Eq. (17) gives the value of ζ_{ij} for any position of $M_{i,j}$, it is always possible to compute and minimize the error $|\zeta_{i,j}|$ by successively moving $M_{i,j}$ between $M_{i-1,j}^{eq}$ and $M_{i+1,j}^{eq}$ along the ψ direction. This gives back the equilibrium position $M_{i,j}^{eq}$ and totally defines δr. Figure 5 illustrates the concept where at each iteration m we use an intermediary displacement δr^m given by

$$\delta\vec{r}^{m} = -\eta_{i,j}^{m}\vec{\zeta}_{i,j}^{m} \quad \text{with} \tag{26}$$

$$\vec{\zeta}_{i,j}^{m} = \left(\frac{1}{r_{i,j}^{m}}\left[\frac{\psi_{i+1}-\psi_i}{r_{i+1,j}^{m}R_{i+1,j}^{eq}} - \frac{\psi_i-\psi_{i-1}}{r_{i,j}^{m}R_{i,j}^{m}}\right] + \left[\mu R\frac{\delta p}{\delta\psi} + \frac{1}{2R}\frac{\delta(F^2)}{\delta\psi}\right]_{i,j}^{m}\right)\vec{e}_{\psi}.$$

The positive multiplicative factor $\eta_{i,j}^{m}$ is a numerical viscosity that controls the speed of the convergence. The orientation of δr^m is the opposite of the unknown displacement's orientation given by Eq. (25). This guarantees that $M_{i,j}^{m}$

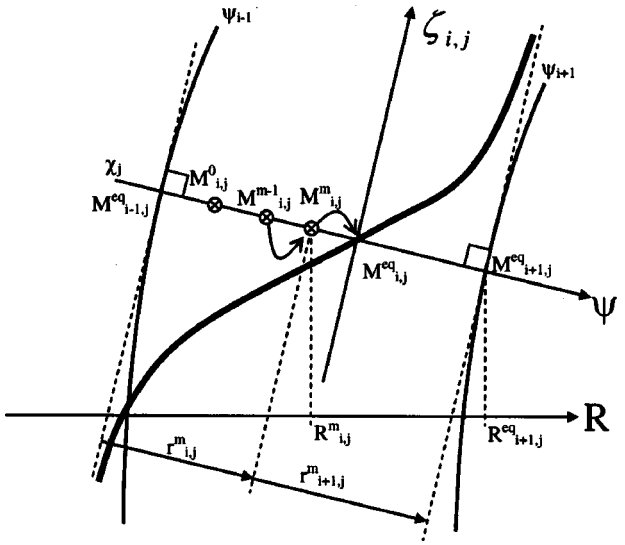

FIG. 5. Successive displacements m of the point $M_{i,j}$ which minimize $|\zeta_{i,j}|$ and give back $M_{i,j}^{eq}$.

moves closer to M_{ij}^{eq} when it is displaced by δr^m. Finally we demonstrated that, for any unknown infinitesimal disturbance introduced in the equilibrium, this iterative method can recover the original configuration by only knowing the position of the disturbed point $M_{i,j}$ relatively to $M_{i-1,j}^{eq}$ and $M_{i+1,j}^{eq}$.

After studying the simple case where a single point is disturbed, we can extend the method to a whole flux line. We can apply a set of unknown infinitesimal displacements (δr_j) to all the points $M_{i,j}$ of a single flux contour i. By applying the preceding principle to this set of points, it is easy to extrapolate that the equilibrium position of the flux contour can be readily obtained.

Finally, in the more realistic case where the whole mesh distribution is far from the equilibrium, the previous idea can be generalized so the series of infinitesimal displacements $(\delta r^0, \delta r^1, \ldots, \delta r^m, \ldots)$ from Eq. (27) will solve the GSh equation for a given p and F,

$$\delta\vec{r}_{i,j}^{\,m} = -\,\eta_{i,j}^m \vec{\zeta}_{i,j}^{\,m} \quad \text{with}$$

$$\vec{\zeta}_{i,j}^{\,m} = \left(\frac{1}{r_{i,j}^m} \left[\frac{\psi_{i+1}-\psi_i}{r_{i+1,j}^m R_{i+1,j}^m} - \frac{\psi_i - \psi_{i-1}}{r_{i,j}^m R_{i,j}^m} \right] + \left[\mu R \frac{\delta p}{\delta \psi} + \frac{1}{2R} \frac{\delta (F^2)}{\delta \psi} \right]_{i,j}^m \right) \vec{e}_\psi. \tag{27}$$

The theory of the calculus of variations demonstrates that this series converges[20] after a finite number m of iterations for a given error ε_m,

$$\varepsilon_m = \max_{i,j} |\zeta_{i,j}| \text{ at the iteration } m. \tag{28}$$

In the preceding paragraphs, we defined the error $\zeta_{i,j}$ in Eq. (17). Then we constructed an error reduction method by studying the behavior of one point, extending it to a whole flux surface, and finally to the whole domain. Equation (27) gives the generic form of the reduction scheme by using infinitesimal displacements. Only the viscosity $\eta_{i,j}$ was left aside, and it is discussed in greater details below.

C. Numerical viscosity definition

The success of the algorithm depends on the control of oscillations arising when the flux lines are moved simultaneously. The numerical viscosity $\eta_{i,j}$ introduced earlier, gives efficient oscillation damping over many plasma configurations, especially at high beta. This viscosity has three components which depend on the iteration m:

(1) a saturation component $\alpha_{i,j}$, preventing flux lines to overlap when moved;
(2) a directional component $\xi_{i,j}$, reducing flux line displacements when the direction of the motion reverses;
(3) a global deceleration component γ, slowing down the flux lines when close to the solution.

The numerical viscosity $\eta_{i,j}$ is a nonlinear directional viscosity.[11] The following discussion deals with each component separately.

The saturation component ensures the integrity of the mesh from one step to the next by preventing a vertex from one line to crossover another line,

$$\alpha_{i,j} = \frac{1}{2} \frac{\min_{k=i+1,i-1} \|M_{i,j} - M_{k,j}\|}{\max_j |\zeta_{i,j}|}. \tag{29}$$

As the convergence approaches, $\zeta_{i,j}$ becomes negligible and this condition is no longer necessary. Thus we can define a maximal positive factor α, which limits the upper values of $\alpha_{i,j}$,

$$\alpha_{i,j} = \min\left(\frac{1}{2} \frac{\min_{k=i+1,i-1} \|M_{i,j} - M_{k,j}\|}{\max_j |\zeta_{i,j}|}, \alpha \right). \tag{30}$$

Keeping the integrity of the mesh is a necessary requirement, but reducing numerical oscillations is also important. At the iteration step m, the directional component takes into account the motion of the point $M_{i,j}$ at the previous steps $m-1$ and $m-2$ to damp oscillations, arising as the motion reverses,

$$\text{If } \delta\vec{r}_{i,j}^{\,m-1} \cdot \delta\vec{r}_{i,j}^{\,m-2} > 0 \quad \text{then at step } m, \xi_{i,j} = 1,$$

$$\text{If } \delta\vec{r}_{i,j}^{\,m-1} \cdot \delta\vec{r}_{i,j}^{\,m-2} < 0 \quad \text{then at step } m, \xi_{i,j} \ll 1. \tag{31}$$

Finally the last component of η_{ij} controls the speed of the convergence. As $\zeta_{i,j}$ diminishes, it is prudent to slow down the convergence to prevent small oscillations around local minima. This technique is known as simulated annealing.[21,22] When repetitious oscillations appear, the value of γ is reduced, pushing further the convergence. An oscillation counter Θ is set up and we have the following condition at the iteration step m:

$$\text{If } \Theta > \Gamma,\ \gamma_m < \tfrac{9}{10}\gamma_{m-1} \quad \text{else } \gamma_m = \gamma_{m-1}. \tag{32}$$

The initial value for γ_0 can be 1. The maximum number of oscillations Γ depends on the geometry of the problem. In general $\Gamma = 10$ gives good results. If Γ is too small, the flux lines will converge to a local minimum; if Γ is too big, the convergence may be jeopardized as oscillations are not damped.

The overall viscosity $\eta_{i,j}$ needs to couple the actions of these three components simultaneously. The simple form retained is given by

$$\eta_{i,j} = \gamma \alpha_{i,j} \xi_{i,j}. \tag{33}$$

This viscosity gives rapid and accurate solutions for both low beta and high beta cases. It provides a robust control of oscillations without preventing fast convergence. The control of the numerical oscillations is hereby resolved. Nevertheless another task still remains. The following paragraphs deal with the consistency between the flux coordinate system and the magnetic flux.

D. Flux correction

The ultimate goal of the algorithm is to find the magnetic flux distribution $(\psi_0, \psi_1 \ldots, \psi_n)$ that suits the input functions p and F. Unfortunately, far from the equilibrium, the flux ψ may not correspond to the actual magnetic flux. Instead ψ should be considered as a regular coordinate which is used in the computational process. Standard methods often compute the flux distribution from the current distribution. Hence the computational flux ψ and the magnetic flux represent the same quantity at each iteration.

On the other hand, the contour dynamics scheme obtains the flux distribution at the iteration m from the one found at the iteration $m-1$ through a set of infinitesimal displacements. Therefore, it is improbable to have a correspondence between the computational flux and the magnetic flux computed from the actual current distribution.

To ensure that the computational flux converges to the magnetic flux, the poloidal induction B_p found in Eq. (4) has to verify Ampère's law, i.e.,

$$\int_{\text{plasma boundary}} \left(\frac{1}{Rh^{\psi}}\right) dl \Bigg|^{m} = \int\int_{\text{plasma}} \left(\mu R \frac{dp}{d\psi} + \frac{1}{2R}\frac{dF^2}{d\psi}\right) dS \Bigg|^{m}. \tag{34}$$

While the flux ψ does not correspond to the actual magnetic flux, Eq. (4) fails to give the poloidal induction and Eq. (34) is not verified. So we have the nontrivial form,

$$\nu^m = \int \left(\frac{1}{Rh^{\psi}}\right) dl \Bigg|^{m} - \int\int \left(\mu R \frac{dp}{d\psi} + \frac{1}{2R}\frac{dF^2}{d\psi}\right) dS \Bigg|^{m}. \tag{35}$$

The factor ν^m can be used to scale the computational flux. This correction has to be infinitesimal to prevent numerical oscillations and the evolution of the flux ψ at the step m is controlled by

$$\psi^m_{\text{total}} = (1 - t^m\ \nu^{m-1})\psi^{m-1}_{\text{total}}, \quad \text{with } t^m \nu^{m-1} \ll 1 \quad \text{and} \quad \psi_{\text{total}} = |\psi_n - \psi_0|. \tag{36}$$

The parameter t^m prevents oscillations caused by the correction ν^{m-1} during the successive iterations. This computation is compatible with Jourdain's variational principle for nonconservative systems.[20] While the variation of ψ is not quite monotonic in this case, it does not violates Jourdain's principle. When we are close to the solution, Eq. (36) becomes quasimonotonic which guarantees theoretical convergence. This correction is not possible with d'Alembert principle, used by Potter,[14] where $\psi_{\text{total}} = |\psi_n - \psi_0|$ has to stay constant throughout the whole equilibrium computation. This scheme implies that the input functions p or F have to evolve during the computation so Ampère's law is satisfied. If one desires to impose input profiles, this flux conserving technique is not appropriate. Furthermore, flux conservation prevents the convergence at high beta.[23] The present algorithm is based on Jourdain's variational principle for nonconservative systems where ψ can vary monotonically. In this case, p and F are kept constant during the computation and the flux ψ varies.

Here we have reached the end of the description regarding the different parts of the contour dynamics scheme for solving high beta equilibria. All the tools described in the preceding paragraphs can now be integrated in the convergence algorithm presented next.

E. Convergence procedure

For given p and F profiles, the algorithm goes as follows:

(1) guess an initial computational flux distribution $(\psi_0, \psi_1, \ldots, \psi_n)$;
(2) compute $\zeta_{i,j}$ for all the points inside the plasma using Eq. (17);
(3) compute $\eta_{i,j}$ for all the points inside the plasma using Eqs. (30)–(32);
(4) correct the flux ψ using Eq. (36) and compute the new distribution $(\psi_0, \psi_1, \ldots, \psi_n)$;
(5) move all the vertices using Eq. (27).

The steps 2 through 5 are repeated until the convergence is achieved, i.e., $\varepsilon_m < \varepsilon_{\max} \ll 1$. The computation time for each vertex is reduced to a minimum, involving only geometrical calculations. This algorithm includes an error calculation, a nonlinear directional viscosity, a flux correction, and a displacement of the grid mesh to reduce the error previously computed. This allows the convergence towards the solution to the GSh equation for the given functions p and F. The following section validates this algorithm by comparing several solutions to analytic or numerical results of the GSh equation, obtained by other methods.

IV. NUMERICAL RESULTS

This section focuses on validating the method presented in this paper. First, we will use an analytic solution of the GSh equation and compare it with the contour dynamics solution. Then, we will define the functions p and F in a manner convenient for code inputs, using polynomials of ψ. Next, we will use numerical solutions to deal with more realistic plasma configurations. Finally, we will present an extreme beta case to demonstrate the versatility of the algorithm. For practical reasons, we will use the geometry of the high aspect ratio Electric Tokamak (ET)[24] at UCLA ($B_\phi = 0.25$ T, $R = 5$ m, $a = 1$ m, $\kappa = 1.5$).

A. Comparison with an analytic solution

To demonstrate the accuracy of the method with simple current distributions, we can compare the equilibria obtained numerically with an analytic solution for high aspect ratio circular plasmas, first investigated by Haas.[25] Because the GSh equation determines the poloidal field, and the toroidal field balances the radial pressure, Haas coupled the pressure and the toroidal function, and introduced a new function f so an analytic solution could be found,

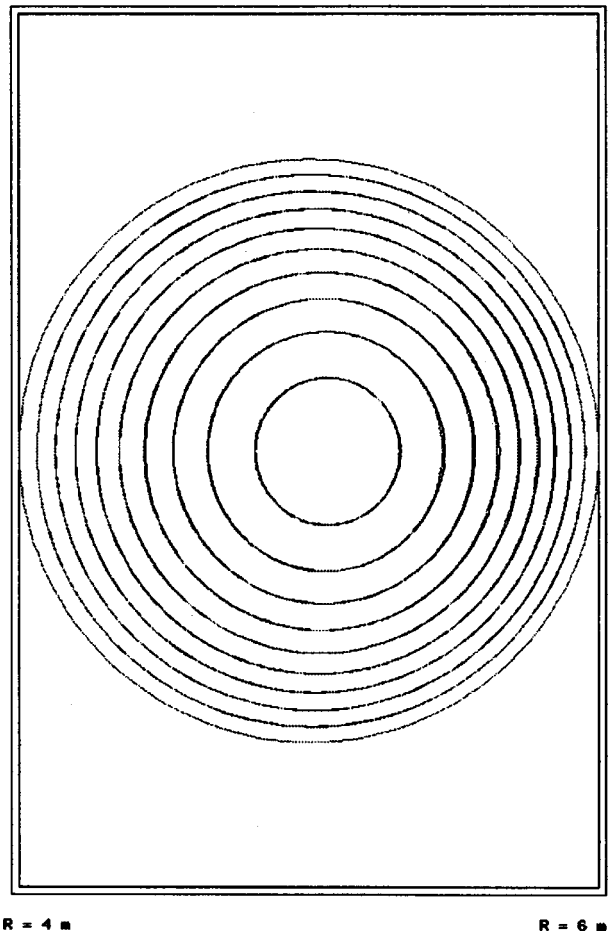

FIG. 6. Comparison between analytic and contour dynamics solutions with 10 flux lines and 140 points per lines. The maximum relative error between the two methods is 0.8% with an average of 0.5%. The two solutions are almost indistinguishable. If more precision is needed, a finer mesh has to be used.

$$F^2(\psi) = R_0^2 B_0^2 \left[1 - \frac{2\mu_0 p(\psi)}{B_0^2} + \frac{2f(\psi)}{B_0} \right]. \tag{37}$$

If we consider p and f linear in ψ, then the solution to the GSh equation is given by

$$\psi(r,\theta) = \frac{A}{4}(r^2 - a^2) + \frac{C}{8}(r^3 - a^2 r)\cos\,\theta,$$

$$\frac{dp}{d\psi} = -\frac{C}{2\mu_0 R_0} \quad \text{and} \quad \frac{df}{d\psi} = -\frac{A}{R_0^2 B_0}, \tag{38}$$

where R_0 is the position of the magnetic axis, a the minor radius, r the distance to the magnetic axis, and θ the angle with the horizontal plane with the magnetic axis as origin. A and C are now the "free functions" of the GSh equation. In Fig. 6, we show comparative results between analytic and numerical solutions. The error stays below 1% with a relatively coarse mesh of 1400 points equally distributed on 10 flux lines. We were able to limit the number of vertices to a minimum because of the quasicircular shape of the flux lines.

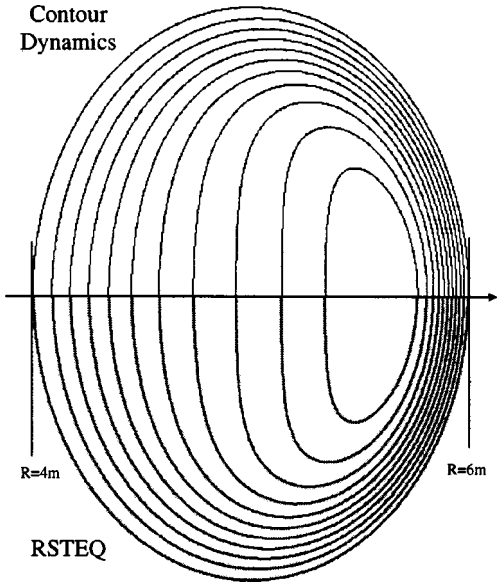

FIG. 7. Comparison between the contour dynamics scheme (top) and RSTEQ (bottom) equilibria for medium average beta, 200 vertices per lines, and 22 flux lines (only 11 lines shown). The maximum error stays below 1.5%.

B. Comparison with a numerical solution

When we depart from simple current distributions, the GSh equation does not have any analytic solution. For the numerical applications of this method, we will consider the input functions p and F as polynomials of the flux, defined as

$$p(\Psi) = p_{\text{boundary}} + \frac{p_{\text{axis}} - p_{\text{boundary}}}{\sum_{i>0} a_i} \sum_{i>0} a_i \Psi^i,$$

$$F^2(\Psi) = F^2_{\text{boundary}} + \frac{F^2_{\text{axis}} - F^2_{\text{boundary}}}{\sum_{i>0} b_i} \sum_{i>0} b_i \Psi^i,$$

$$\Psi = \frac{\psi - \psi_{\text{boundary}}}{\psi_{\text{axis}} - \psi_{\text{boundary}}}. \tag{39}$$

It is very convenient to use such forms for p and F because this concise decomposition can match a lot of real plasma configurations.

We have calculated several types of equilibria using the "direct-type solver" resistive stability toroidal equilibrium (RSTEQ) code[26] developed at the Oak Ridge National Laboratory. It can be used rather efficiently to benchmark the present method at average betas, i.e., below 20%. The equilibrium profiles p, F, and ψ were computed using the contour dynamics scheme. They were used as inputs to the RSTEQ code to check the consistency of the results. In Fig. 7, we present a comparison between the two methods. The error does not go above 1.5% with a relatively coarse mesh of 4400 nodes.

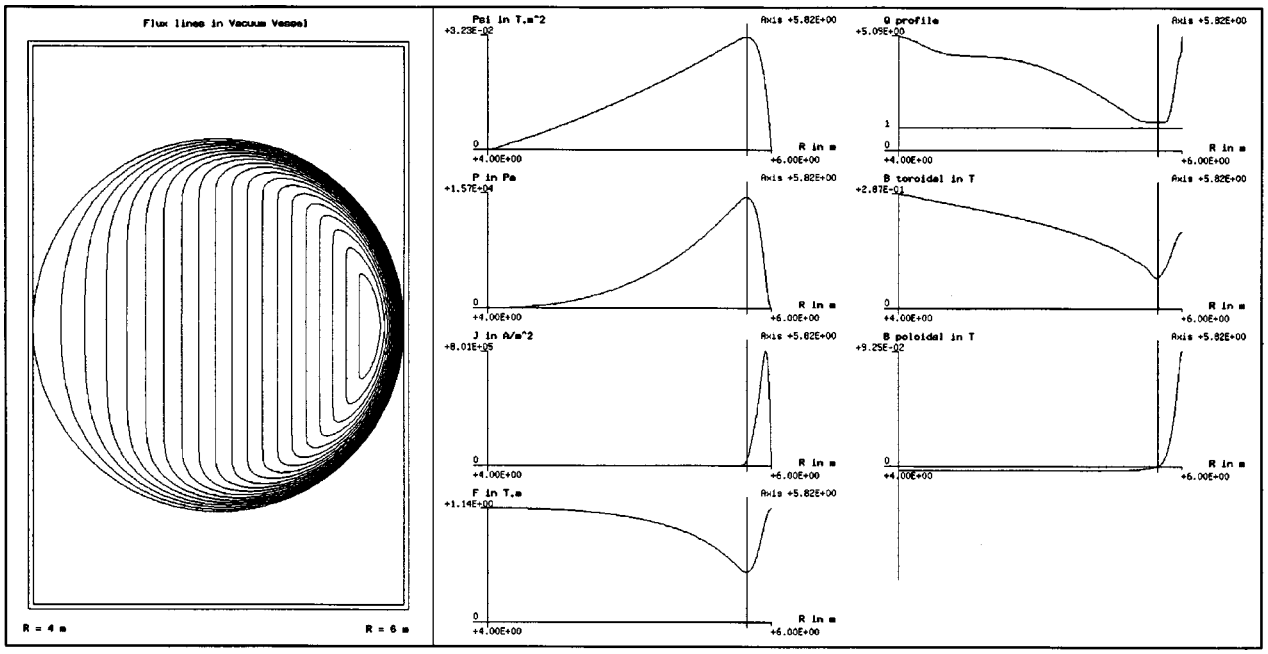

FIG. 8. An extreme equilibrium with an average beta of 27% (100% peak beta, 8.1 poloidal beta) for a circular-shaped plasma of 175 kA and a mesh with 20 flux lines and 200 vertices per line.

C. High beta case

For high beta, few codes achieve good performances.[9] As the flux lines get squeezed on the low field side, linear system inversion becomes difficult and successive errors tend to increase. The method presented does not include such mathematical techniques and is designed to diminish successive errors. So convergence exists for a wide range of boundary shapes and current profiles.

If we take equilibria with extreme Shafranov shift, inspired by Cowley,[16] the code converges for shifts greater than 80% at unity peak beta, as shown in Fig. 8. The core solution and boundary layer[27] are clearly visible. Inside the core, the flux lines depend on R only. It should be noted that the only stability criterion applied to this equilibrium is $q>1$. Here we do not present stable or unstable configurations but equilibrium solutions that demonstrate code capabilities. Other shaped equilibria can be readily computed using this method. Here we have presented only the classical circular version of high beta plasmas.

V. CONCLUSION

This work has described a method for solving the Grad–Shafranov equation. It uses the contour dynamics approach to simplify the mathematical tools to resolve this nonlinear problem. By combining a variational principle with an adequate coordinate system readjustment, high, hence low, beta plasma equilibria can be computed over a wide range of fixed boundary shapes. To obtain reliable results, strict convergence control is enforced using a nonlinear directional viscosity. Convergence is very fast for standard plasma beta and remains adequate as beta is increased toward unity. Solutions can be found for Shafranov shifts which correspond to a substantial fraction of the minor radius. We note that such equilibria have eluded RSTEQ when increasing plasma beta through a flux conserving sequence.[23] Even though this is beyond the scope of this paper, we add that the method can be readily extended to free boundary equilibria at high plasma beta.[11]

ACKNOWLEDGMENTS

One of the authors (P.A.G.) would like to thank L. Krähenbühl, Ecole Centrale de Lyon, France for his help and support throughout the research on this topic and R. J. Taylor, University of California, Los Angeles, USA, for his insight and advice on high beta plasma physics.

This work was supported at UCLA by the U.S. Department of Energy, Grant No. DE-FG03-01ER54617.

APPENDIX: GRADIENT AND CURL OPERATORS

In an orthogonal system (e_1,e_2,e_3) with coordinates (q_1,q_2,q_3) and metric (h_1,h_2,h_3), we have

$$\vec{\nabla} U = \frac{1}{h_1}\frac{\partial U}{\partial q_1}\vec{e}_1 + \frac{1}{h_2}\frac{\partial U}{\partial q_2}\vec{e}_2 + \frac{1}{h_3}\frac{\partial U}{\partial q_3}\vec{e}_3, \tag{A1}$$

$$\vec{\nabla}\times\vec{A} = \frac{1}{h_2h_3}\left(\frac{\partial(h_3A_3)}{\partial q_2} - \frac{\partial(h_2A_2)}{\partial q_3}\right)\vec{e}_1 + \frac{1}{h_2h_3}\left(\frac{\partial(h_1A_1)}{\partial q_3} - \frac{\partial(h_3A_3)}{\partial q_1}\right)\vec{e}_2 + \frac{1}{h_1h_2}\left(\frac{\partial(h_2A_2)}{\partial q_1} - \frac{\partial(h_1A_1)}{\partial q_2}\right)\vec{e}_3. \tag{A2}$$

[1] F. Chen, *Introduction to Plasma Physics and Controlled Fusion*, 2nd ed. (Plenum, New York, 1984).
[2] V. D. Shafranov, *Reviews of Plasma Physics* (Consultants Bureau, New York, 1966), Vol. 2, pp. 103–151.
[3] K. Lackner, Comput. Phys. Commun. **12**, 33 (1976).

[4]J. Blum, J. L. Foll, and B. Thooris, Comput. Phys. Commun. **24**, 235 (1981).
[5]J. D. Callen and R. A. Dory, Phys. Fluids **15**, 1523 (1972).
[6]G. O. Ludwig, Plasma Phys. Controlled Fusion **39**, 2021 (1997).
[7]J. DeLucia, S. C. Jardin, and A. M. M. Todd, J. Comput. Phys. **37**, 183 (1980).
[8]L. L. Lao, S. P. Hirshman, and R. M. Wieland, Phys. Fluids **24**, 1431 (1981).
[9]L. E. Zakharov and A. Pletzer, Phys. Plasmas **6**, 4693 (1999).
[10]R. Gruber, R. Iacono, and F. Troyon, J. Comput. Phys. **73**, 168 (1987).
[11]P.-A. Gourdain, Ph.D. thesis, 2001, Ecole Centrale de Lyon, No. ECL 2001-33.
[12]N. J. Zabusky, M. H. Hughes, and K. V. Roberts, J. Comput. Phys. **135**, 220 (1997).
[13]H. L. Berk and K. V. Roberts, Methods Comput. Phys. **9**, 87 (1967).
[14]D. E. Potter, Methods Comput. Phys. **16**, 43 (1976).
[15]M. N. Rosenbluth, D. A. Monticello, H. R. Strauss, and R. B. White, Phys. Fluids **19**, 1987 (1976).
[16]S. C. Cowley, P. K. Kaw, R. S. Kelly, and R. M. Kulsrud, Phys. Fluids B **3**, 1468 (1991).
[17]J. P. Friedberg, *Ideal Magnetohydrodynamics* (Plenum, New York, 1987), p. 110.
[18]J. Blum, *Numerical Simulation and Optimal Control in Plasma Physics* (Wiley, New York, 1989).
[19]L. L. Lao, Comput. Phys. Commun. **31**, 201 (1984).
[20]B. D. Vujanovic and S. E. Jones, *Variational Method in Non Conservative Phenomena* (Academic, Boston, 1989), pp. 123–129.
[21]S. Kirkpatrick, C. D. Gelatt, and M. P. Vecchi, Science **220**, 671 (1983).
[22]S. Kirkpatrick, J. Stat. Phys. **34**, 975 (1984).
[23]M. W. Kissick, J. N. Leboeuf, and S. E. Kruger, Phys. Plasmas **10**, 1060 (2003).
[24]R. J. Taylor, J.-L. Gauvreau, M. Gilmore, P.-A. Gourdain, D. J. LaFonteese, and L. W. Schmitz, Nucl. Fusion **42**, 46 (2002).
[25]F. A. Haas, Phys. Fluids **15**, 141 (1972).
[26]J. A. Holmes, Y.-K. M. Peng, and S. J. Lynch, J. Comput. Phys. **36**, 35 (1980).
[27]S. C. Hsu, M. Artun, and S. C. Cowley, Phys. Plasmas **3**, 266 (1996).